Journal of Dynamics, Monitoring and Diagnostics, 2022, 1, 169-175
https://doi.org/10.37965/jdmd.2022.85

ISTP
RESEARCH ARTICLE

Intelligent Identification of Rotating Stall for Centrifugal Compressor Based on Pressure Pulsation Signals and SDKAE Network

Hongkun Li, Jiayu Ou, Xinwei Zhao, Hongwei Cao, and Daitong Wei
School of Mechanical Engineering, Dalian University of Technology, Dalian 116000, China

(Received 27 February 2022; Revised 15 June 2022; Accepted 02 August 2022; Published online 02 August 2022)

Abstract: Most accidents of centrifugal compressors are caused by fluid pulsation or unsteady fluid excitation. Rotating stall, as an unstable flow phenomenon in the compressor, is a difficult point in the field of fluid machinery research. In this paper, a stack denoising kernel autoencoder neural network method is proposed to study the early warning of rotating stall in a centrifugal compressor. By collecting the pressure pulsation signals of the centrifugal compressor under different flow rates in engineering practice, a double hidden layer sparse denoising autoencoder neural network is constructed. According to the output labels of the network, it can be judged whether the rotation stall occurs. At the same time, the Gaussian kernel is used to optimize the loss function of the whole neural network to improve the signal feature learning ability of the network. From the experimental results, it can be seen that the flow state of the centrifugal compressor is accurately judged, and the rotation stall early warning of the centrifugal compressor at different speeds is realized, which lays a foundation for the research of intelligent operation and maintenance of the centrifugal compressor.

Key words: centrifugal compressor; deep learning; pressure pulsation signal; rotating stall

I. INTRODUCTION

Centrifugal compressor has the advantages of compact structure, durability, and high-pressure ratio, and there is a lot of research on targeted applications in the corresponding fields [1,2]. In the past, the research on centrifugal compressors mainly focused on aerodynamic aspects, and the main goal of this research work was to improve efficiency, pressure ratio, and operating range [3]. However, with the improvement of aerodynamic performance, the limitation of mechanical capacity in the design of centrifugal compressors has appeared concurrently. Therefore, while achieving higher aerodynamic performance, it is also very important to ensure the safe operation of the machine and avoid mechanical failure.

Rotating stall is an important fault during the operation of a centrifugal compressor [4,5]. When the operating point is far away from the design working condition, the airflow can be separated in the flow channel, resulting in an unstable flow of the working fluid. Aerodynamic pressure pulsation in the machine flow channel and pipeline may follow and lead to a flow-induced vibration of impeller, causing great harm to the machine [6,7]. Therefore, it is of great significance to study the critical flow value of rotating stall of centrifugal compressor to improve the stability of industrial centrifugal compressor.

At present, the research on compressor rotating stall state identification mainly focuses on time-domain analysis, frequency domain analysis, polar graph, time-frequency analysis, and chaos theory analysis. Ali Zamiri et al. [8] used the scale-adaptive simulation method to predict and capture the key characteristics of rotating stalls in transonic high-pressure centrifugal compressors. By comparing the unsteady pressure signal with the measured data, the reliability of the proposed numerical model for rotating stall prediction is verified. Zhang et al. [9] processed the pressure signals using the coherence analysis method, and the unsteady evolution principle of the rotating stall is revealed in more detail. The experimental results reveal that the rotating stall has a major impact on the unsteady pressure signal, which is mainly manifested in the increase of pressure pulsation. Adel Ghenaiet et al. [10] demonstrated the potential of numerical simulation to plot the whole flow field and evaluated some criteria for predicting the onset of stall. The determination of the flow value of the rotating stall plays an important role in the safety and control of a centrifugal compressor operating under a high-pressure ratio. Lu et al. [11] explained the generation mechanism and inducement of the rotating stall. At the same time, a vibration method based on flow state identification (FSIV) is presented to discover the flow instability in a centrifugal pump. Zhao et al. [12] used a strain gauge and tip timing sensor to monitor blade vibration, and the pressure sensor based on circumferential distribution and stall parameter identification method is explored. At present, most of the research on rotating stalls of a centrifugal compressor is in time-frequency domain numerical analysis such as the coherence analysis method. With the development of intelligent manufacturing, the analysis ability of these models is obviously insufficient in the face of massive engineering data in actual processing [13].

In this paper, a stacked denoising kernel autoencoder neural network is proposed to identify the rotating stall state of a centrifugal compressor. The deep learning method is used to deeply extract the pressure signal of a centrifugal compressor by constructing a multi-hidden layer autoencoder neural network. The Gaussian kernel is adopted to modify the loss function term to accurately judge the critical value of the rotating stall. Through analyzing the pressure signals of 11 different flow conditions, the critical flow value of the rotating stall is accurately determined.

Corresponding author: Hongkun Li (e-mail: lihk@dlut.edu.cn)

II. PROPOSED METHOD

Autoencoder is a model that automatically learns features from the collected data and provides a better feature representation to replace the raw signals [14]. In practical application, the features extracted by a sparse encoder can be used to replace the original signals, which can often bring better results [15]. For a data sample size $m \times n$ dimensional, $X = [X_1, X_2, \cdots X_n] \in R^{m \times n}$, among them $X_i = [x_1, x_2, \cdots x_m] \in R^{m \times 1}$. The information of the hidden layer $H = [h_1, h_2, \cdots h_d] \in R^{d \times 1}$ is represented as:

$$h = f(Wx + b) \tag{1}$$

where f is a neuron nonlinear function, and sigmoid function is commonly used. W is a weight parameter size $d \times m$ dimension. b is the offset value size $d \times 1$ dimension. The output layer reconstruction signals Z can be written as:

$$z = f(W'h + b') \tag{2}$$

where W' and b' are the parameter-connected hidden layer and the output layer, respectively. The size of parameter W' is $m \times n$ dimension, and b' is $m \times 1$ dimension.

The number of input and output nodes of the autoencoder model is the same, and if the number of nodes in the hidden layer is smaller than the number of input nodes, the sample is compressed, that is, the features of the sample are extracted. Meanwhile, the output of the neural network is required to restore the input layer as much as possible, that is, the difference between output and input is as small as possible [16,17]. So the loss function can be expressed as:

$$E(p) = \frac{1}{2}\sum_{i=1}^{m}(z_i - x_i)^2 \tag{3}$$

In order to enhance the feature extract ability of neural networks and reduce the interference of environmental noise on processing signals, the function of signals noise reduction is added to the autoencoder model [18]. Meanwhile, the sparsity limitation of neural network is to represent the test samples with the least elements as much as possible. Therefore, the sample signals will be randomly assigned 0. Sparsity can be expressed as [19]:

$$KL(\rho \| \widehat{\rho}_j) = \rho \log \frac{\rho}{\widehat{\rho}_j} + (1-\rho)\log \frac{1-\rho}{1-\widehat{\rho}_j} \tag{4}$$

$$\widehat{\rho}_j = \frac{1}{m}\sum_{i=1}^{m}[a_j^{(2)} X_i] \tag{5}$$

where $a_j^{(2)}$ indicates the activation degree of hidden neuron j when the input data is X. $\widehat{\rho}_j$ is the average activated data. In order to make the average activation degree a small value, ρ is introduced, which is called sparsity parameter and satisfies $\widehat{\rho}_j = \rho$, so that the activity of hidden layer nodes can be small.

A. IMPROVED LOSS FUNCTION

Based on the fault identification principle, the linearly nonseparable sections in low-dimensional space could be linearly separable if mapping into the high-dimensional space. Nevertheless, if this technology is directly applied for identification and classification, there will exist many problems, like determining the dimension of feature space and the parameters of nonlinear mapping function [20]. The biggest challenge is the "dimension disaster" in the high-dimensional space operation. Kernel function technology gives an elegant solution. Supposing $x \in X$, samples in $R(n)$ space. There is a nonlinear function φ that maps input sample X to feature space F. Where the dimension of F is $R(m)$, which is satisfied n ≪ m. This transformation process can be written as:

$$K(x,z) = \langle \varphi(x), \varphi(z) \rangle \tag{6}$$

where $\langle , \rangle$ is a function of inner product. From the formula (6), inner product is used by the kernel function to cleverly handle the problems of "dimensionality disaster" in the high-dimensional feature spaces.

The kernel function has the following properties [21]: (1) the use of the kernel function effectively avoids the problem of "dimension disaster" of high data and greatly reduces the amount of calculation. Therefore, kernel function model can effectively handle high-dimensional input data problems. (2) It does not even need to acquaint the form and parameters value of the function Φ. (3) Kernel technology combined with other classification algorithms can form different methods based on kernel function technology to apply to different applications, and the construct of these two sections can be carried out separately.

Gaussian kernel, also known as radial basis function (RBF), is a commonly used kernel function [22]. It can map finite-dimensional data to high-dimensional space. For any two random signal samples $x = [x_1, x_2, \cdots, x_N]^T$ and $z = [z_1, z_2, \cdots, z_N]^T$, the function of Gaussian kernel is expressed as:

$$k_\sigma(x_i, z_i) = \frac{1}{\sqrt{2\pi}\sigma}\exp\left(-\frac{(x_i - z_i)^2}{2\sigma^2}\right) \tag{7}$$

where σ is the kernel size. Thus, the final loss function with a Gaussian kernel can be reconstructed as:

$$E(p) = \frac{1}{m}\sum_{i=1}^{m} k_\sigma(x_i - z_i) \tag{8}$$

To avoid the over-fitting problem in the feature learning process, a weight attenuation function J_{weight} is used to restrict the loss function, and its expression is as follows:

$$J_{\text{weight}} = \frac{\lambda}{2}\sum_{l=1}^{2}\sum_{i=1}^{s_l}\sum_{i=1}^{s_{l+1}}(W_{ji}^{(l)})_i^2 \tag{9}$$

where λ is the weight adjust parameter and s_l is the unit number of l layers.

Therefore, the whole loss function of the proposed method is as follows:

$$L(p) = E(p) + J_{\text{weight}}(p) + KL(\rho \| \widehat{\rho}_j) \tag{10}$$

B. GENERAL PROCEDURE

In this paper, SDKAE is proposed to intelligently diagnose the critical flow of rotating stall of centrifugal compressor. SDKAE belongs to an unsupervised deep learning method. It can effectively extract features from raw signals and provide better feature information than the original data. The main goal of unsupervised learning is to deeply mine the structure and internal information of data group. According to the length of the collected signals, the pressure fluctuation signals at each flow rate is transformed into

200 samples, and each sample contains 2048 signal points. The total number of samples at 11 flow rates is 2200. Therefore, the final sample size of the neural network is 2200×2048. The flowchart of the proposed method is displayed in Fig. 1. The main implementation steps can be concluded as follows:

1. The pressure signals of 11 different flows of centrifugal compressor are collected. Through the pressure signal processing, the one-dimensional time-domain signal is made into 2200×2048 signal samples, including 11 flow conditions
2. A stack denoising kernel autoencoder neural network with two hidden layers is constructed, leveraging the learning capability of unsupervised learning models for signal feature information. The loss function is modified with Gaussian kernel function, and white noise is added to initialize the parameters of the network.
3. The softmax classifier is added to the end of the network in the previous step to form a supervised model. The pressure pulsation signals are used as the input sample of neural network. Through multiple iterative learning, the flow state of the pressure pulsation signal is identified and the rotating stall flow is determined.

III. EXPERIMENTAL SETUP

A. COMPRESSOR TEST RIG

Experiments were conducted using a single-stage centrifugal compressor facility. This compressor was designed and built to allow detailed investigations of the fundamental flow physics and aeromechanical interaction within centrifugal compressors. Figure 2 demonstrates the test rig and flow path of the compressor.

The major components of the facility include the inlet and outlet ducting, blade sections, electric motor, drive train, and instrumentation. The facility is operated in an open cycle. The air is first sucked in from long pipe system and the inlet flow boundary corresponds to ambient conditions. Afterward, the flow is guided and entered into the compressor. Along the flow path, variable inlet guide vanes (VIGVs), a full-size unshrouded impeller, diffuser vanes (DVs), and return channel vanes can be seen. The blade count of each component is listed in Table I. The tested impeller is a typical unshrouded one and normally operates at high tip speed and large volume flow. With 2.1 MW electric motor, the impeller is driven to the required operating speed via a 2.93 ratio gearbox. The nominal rotor blade tip gap is 0.5% of the leading edge (LE) impeller blade span.

B. INSTRUMENTATION AND OPERATION POINT MEASUREMENT

Total pressure rakes and total temperature rakes are installed in the inlet and outlet ducting. These instruments provide important tools for configuring and monitoring the operating conditions of the compressor stage. A flow meter is installed on the outlet pipe to monitor the operating mass flow rate. The characteristic map for compressor stage at

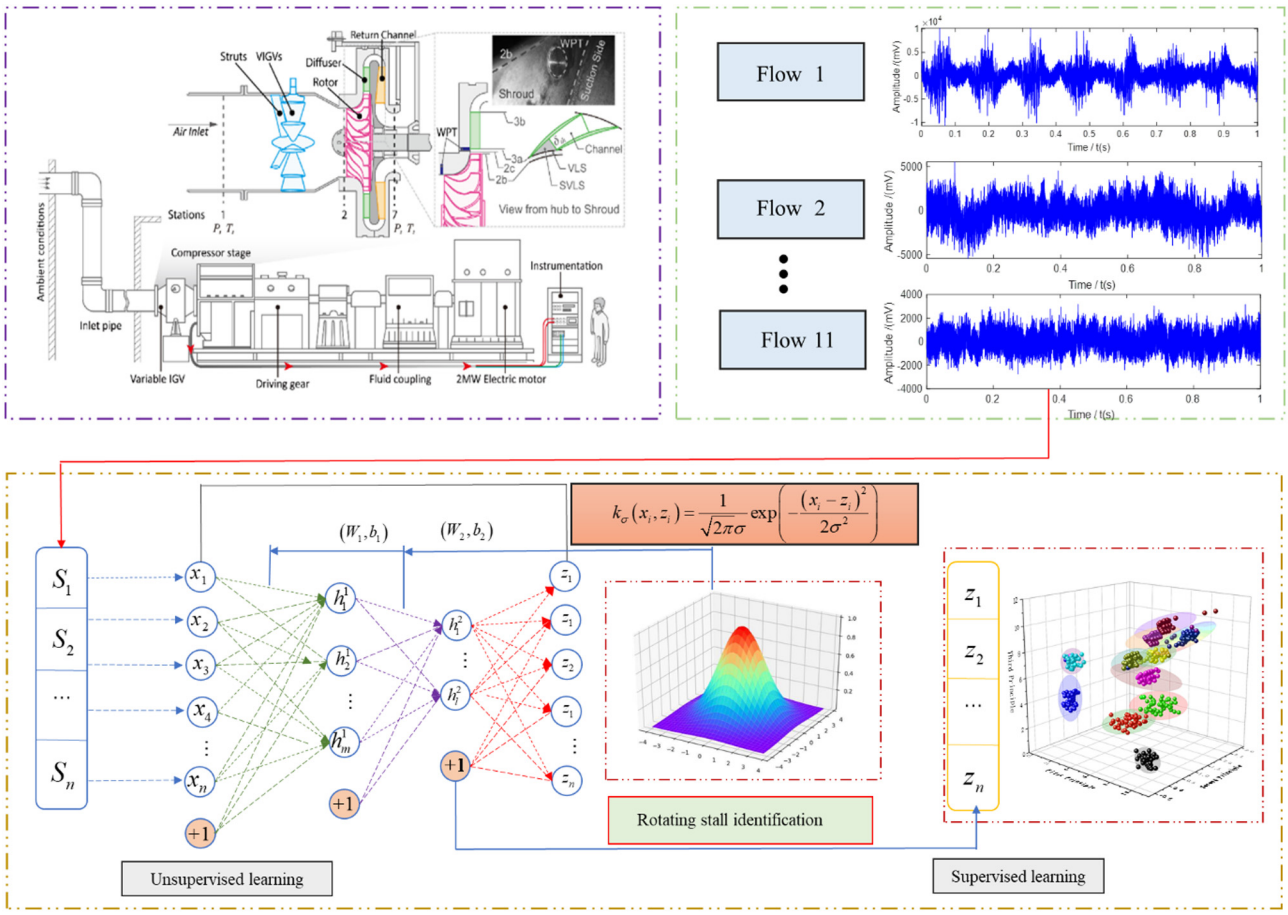

Fig. 1. The proposed method implementation steps.

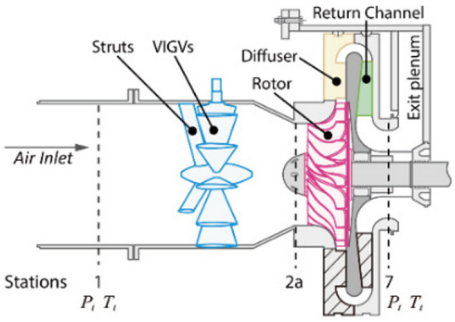

Fig. 2. Schematic diagram of test bench.

TABLE I Blade counts of the tested compressor rig

Row	VIGVs	IMP	DV	RC
Number	11	19	20	18

different constant rotating speeds was tested in detail during previous study. Any mass flow point on the performance line is tested for a long period to well attain the performance with low relative error and uncertainty. Considering the inlet condition change due to open cycle facility, the corrected mass flow is used and can be calculated from

$$\dot{m}_{\text{cor}} = \dot{m}\frac{P_{\text{ref}}}{P_{t,0}}\sqrt{\frac{T_{t,0}}{T_{\text{ref}}}}$$

$$\text{with} \quad P_{\text{ref}} = 1.01325\,\text{bar}, \qquad T_{\text{ref}} = 288.15\text{K} \tag{11}$$

where $\dot{m}$ is the mass flow rate, $P_{t,0}$ is the total pressure, and $T_{t,0}$ is the total temperature at the compressor inlet, and P_{ref} and T_{ref} are a reference pressure and reference temperature, respectively. Then, the stage total pressure ratio and isentropic efficiency are written by:

$$\Pi^{t-t} = \frac{\bar{P}_{t,7}}{\bar{P}_{t,1}}, \qquad \eta_{is} = \frac{\Pi^{t-t\frac{\kappa-1}{\kappa}} - 1}{\frac{T_{t,7}}{T_{t,1}} - 1} \tag{12}$$

as a function of the corrected mass flow in Eq. (11). Due to confidentiality restrictions, the design quantities and some compressor parameters will not be listed here, and only normalized values are provided, which is enough for current research. The normalized operating speed Ω_{norm} of the centrifugal compressor is defined as a percent of normal speed Ω_{Nn} which corresponds to the first speed line and is also denoted in Fig. 3(a) with N100:

$$\Omega_{\text{norm}} = \Omega_{\text{rot}}/\Omega_{\text{Nn}} \tag{13}$$

where Ω_{rot} is the rotational speed of the impeller. The compressor characteristic curve is illustrated in Fig. 3. Performance parameters are normalized by the designed mass flow rate $\dot{m}_{\text{design}}$, total pressure ratio $\Pi^{t-t}{}_{\text{design}}$, and isentropic efficiency $\eta_{\text{is,design}}$ (aerodynamic design point at N100).

C. TRANSIENT WALL PRESSURE MEASUREMENT

Unsteady instrumentation is also utilized for this work. High-frequency wall pressure transducers are inserted into the shroud casing for flow field measurements. These

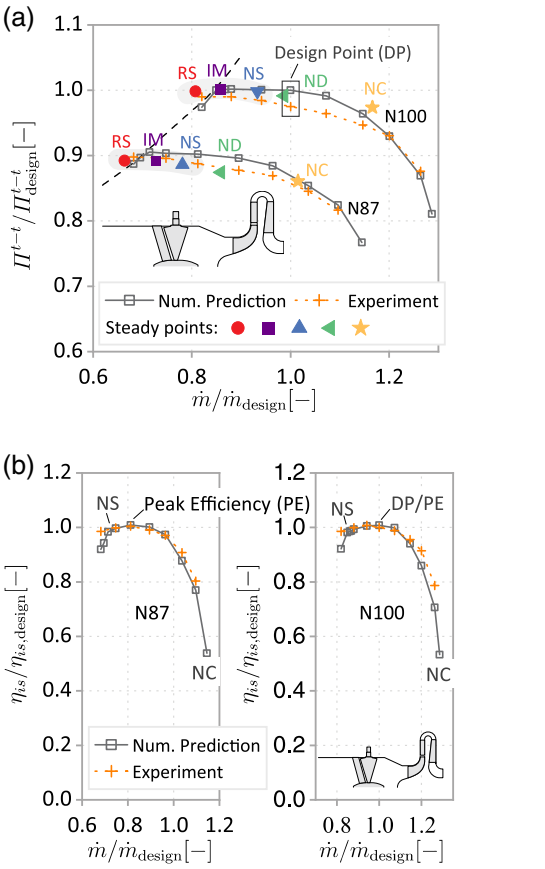

Fig. 3. Performance map for compressor rig and tested operating points.

pressure sensors used in the experiments are piezoelectric sensors made by PCB Piezotronics (Model 106B52). A circumferential array of five high-frequency pressure sensors (P1–P5), located upstream of the diffuser vane LE, are flush-mounted to the flow surface of the shroud. Additional sensors are uniformly distributed within one diffuser flow passage from vane inlet (LE, 0% location) to outlet (TE, 100% location) at the middle region (50%VP location) of the diffuser channel. Detailed spatial locations of the sensors can be found in Fig. 4.

All pressure signals are recorded synchronously using a dedicated acquisition card, which is used for multichannel

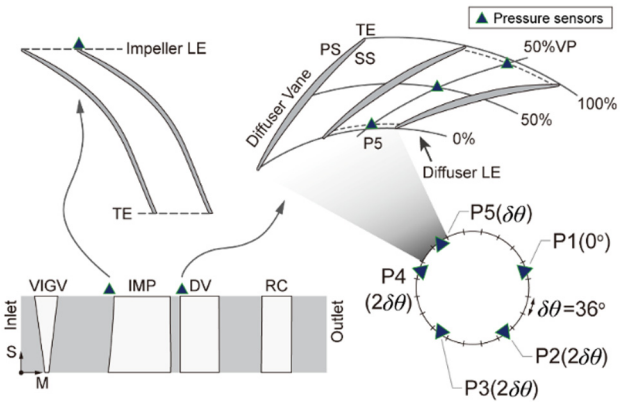

Fig. 4. Wall pressure transducer arrangement within the compressor flow passage.

high-precision measurement. The pressure fluctuation signals from multiple wall pressure sensors are acquired simultaneously during the experiment. In order to well resolve the characteristic frequency and the timescale of interest, the sampling rate is 20.48 kHz, which provides enough signals to resolve the rotating stall frequency (RSF) and the blade passing frequency (BPF) The accuracy of the dynamic measurement is verified from the perspective of reproducibility using redundancy tests. These pressure signals are then used to study the rotating stall and further predict the internal flow condition.

IV. RESULT AND ANALYSIS

In this paper, a stack denoising kernel autoencoder neural network method is proposed to intelligently determine the operating condition of the investigated centrifugal compressor, especially the rotating stall. The training process parameters and data samples of the proposed model are shown in Table II. As stated before, 11 different mass flow points in total are measured which mostly covers the entire operating flow range. At each speed line (N100 and N87), five operating points from system choked flow to stall boundary, namely near choke (NC), near design (ND), near stall (NS), intermediate (IM), and rotating stall (RS), respectively, are investigated. These operation points are also denoted in Fig. 3. Attribute to the variation of blade aerodynamic loading condition, the internal unsteady flow changes accordingly, leading to different wall pressure fluctuation characteristics. The surge point followed by a rotating stall at N100 speed is also considered, which represents the 11th operating condition. With these measurement dates, the compressor flow condition along the flow path can be well described.

TABLE II Parameters of the proposed model

Parameters	Value
Input size	2048
Hidden sizeL1	400
Hidden sizeL2	200
Sparsity	1
Weight decay	3e-5
weight penalty	1
Noise intensity	0.3
Training samples	130
Testing samples	70

In order to avoid the contingency of one experimental result, five repeated experiments were carried out, and the experimental accuracy is shown in Table III. It can be seen from Table III that only at the speed N100, the identification accuracy of RS flow is 70%–80%, the other flow identification accuracy is more than 80%, and the highest flow identification accuracy can reach 100. The recognition accuracy of RS at N87 speed with rotating stall is

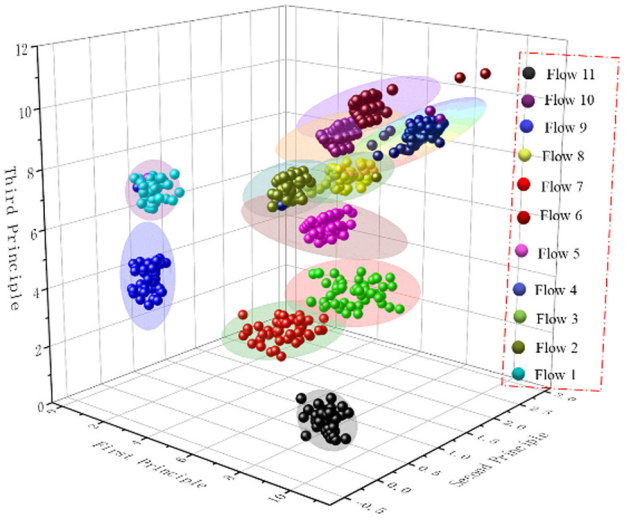

Fig. 5. Three-dimensional clustering results of pressure fluctuation signals.

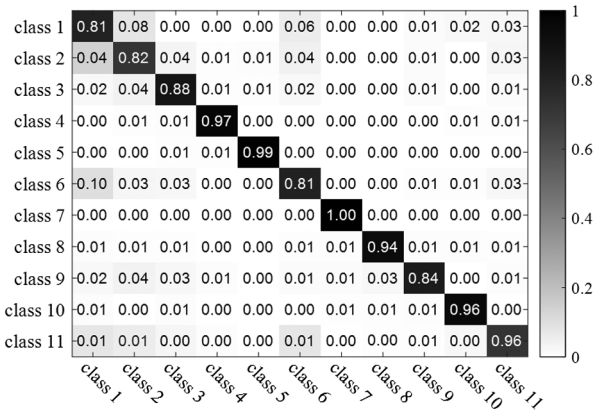

Fig. 6. Confusion matrix between the predicted value and real value of flow state of pressure pulsation signal.

TABLE III Identification accuracy of each flow rate in five tests

	N100						N87				
Operation points	Surge	RS	IM	NS	ND	NC	RS	IM	NS	ND	NC
Class	1 (%)	2 (%)	3 (%)	4 (%)	5 (%)	6 (%)	7 (%)	8 (%)	9 (%)	10 (%)	11 (%)
Test 1	82	84	79	97	99	79	100	96%	80	92	82
Test 2	82	80	78	100	97	78	100	97%	89.5	91.5	94
Test 3	80.5	82	88	97.5	99	81	100	94.5%	84	96	96
Test 4	87	86.5	80.5	96.5	98.5	82.5	100	95.5%	88	95	95
Test 5	80	83	79.5	97.5	100	80.5	100	95	84%	97	97

97%. The average accuracy reaches 90.75%, meeting the needs of production and processing. It provides a basis for knowing the signal of the rotating stall of centrifugal compressor.

In order to more intuitively show the identification of pressure pulsation signals at different flow rates, the three-dimensional graph clustering method is adopted to show the aggregation of pressure pulsation signals at different flow rates. The experimental results are shown in Fig. 5. In Fig. 5, the balls of each color represent the pressure pulsation signal under one flow rate. It can be seen from the figure

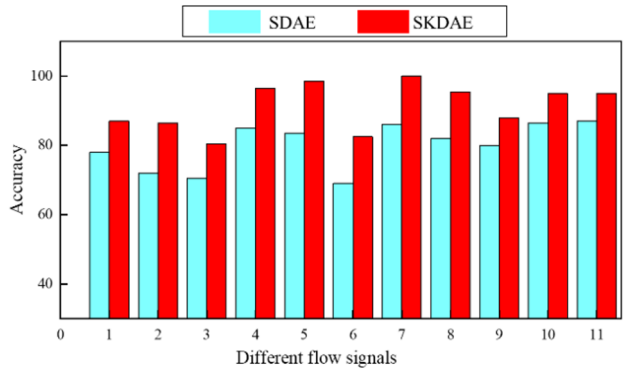

Fig. 7. Comparison results of SKDAE and SDAE.

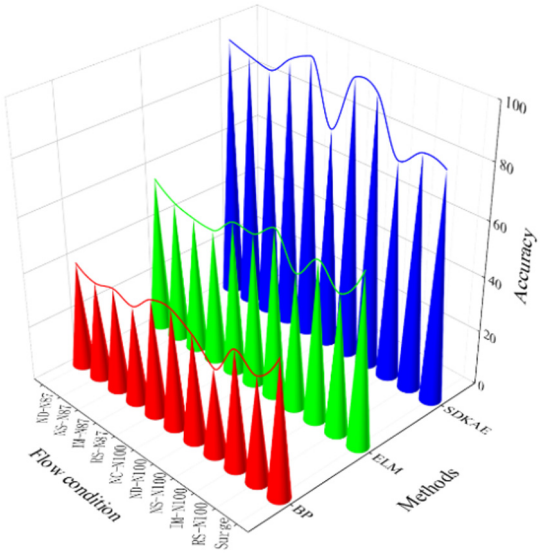

Fig. 8. Accuracy comparison results of different methods.

that the signal aggregation effect under five flow rates is the best, almost completely separated, and the remaining pressure pulsation signals, despite individual mixing, still achieve a good classification effect.

A confusion matrix, usually called error matrix, is the most intuitive and concise method to evaluate accuracy. Diagonal elements are usually used to represent the difference between the predicted value and the real value of the model. This paper also uses the confusion matrix method to show the comparison between the prediction results of the pressure pulsation signal flow state and the real value. The results are shown in Fig. 6, and the diagonal number is the accuracy of the prediction results. From the results, it can be concluded that the model predicted results of other flow states are more than 80%, and the highest predicted value of flow state is 100%.

In order to verify the effectiveness of Gaussian kernel function in enhancing the performance of a neural network, the method of comparative experiment is adopted. The standard SDAE network without Gaussian kernel function is selected as the comparative method. The comparative experimental results are shown in Fig. 7. It can be seen from the experimental results that the accuracy of SKDAE is higher than that of SDAE for the identification of pressure fluctuation signals under 11 flow conditions, which proves that Gaussian kernel function has an obvious effect on signal feature extraction.

In order to verify the accuracy of this method in identifying the flow state of pressure pulsation signal of a centrifugal compressor, a comparative experimental method is adopted. The typical extreme learning machine (ELM) model and backpropagation (BP) neural network are selected for the comparison methods. The identification results of each flow state are shown in Fig. 8. Also, the comparison research with the current widely used frontier methods including convolutional neural networks (CNNs), long- and short-term memory networks (LSTMs), and online extreme learning machines (OSELMs) was conducted, and the experimental results are shown in Table IV. All comparative experiments need to emphasize that all the data processed by the comparative methods and the proposed model in this paper are the collected original signals. The process of making input samples is exactly the same, and there is no human intervention in the experiment. In order to ensure the reliability of the experimental results, all the listed results are the average accuracy.

The experimental results show that the accuracy of the proposed model is higher than that of the comparison methods, which further demonstrated the advantages of stacked denoising kernel autoencoder neural network in pressure pulsation signal flow identification.

TABLE IV Comparison of experimental results

	Flow										
Method	**1**	**2**	**3**	**4**	**5**	**6**	**7**	**8**	**9**	**10**	**11**
SDKAE	87	86.5	80.5	96.5	98.5	82.5	100	95.5	88	95	95
CNN	56.5	65.2	62.5	70.5	71	65	70.5	68	62.5	67	65
LSTM	89	82	78	94.5	96.5	78	95	92	82	89	92.5
OSELM	83	80	78	92	83.5	82	93.5	87	79.5	78	86

V. CONCLUSION

In this manuscript, a stacked denoising kernel autoencoder neural network is proposed to identify the rotating stall state with pressure pulsation signals of centrifugal compressor. Gaussian kernel function is applied to reconstruct the whole loss function of the proposed model, and Gaussian white noise is added to enhance the feature extraction ability to pressure pulsation signals. Through the state identification of the pressure pulsation signals collected under two rotating speeds and 11 flow conditions, the flow state of the pressure pulsation signal can be accurately judged. The recognition accuracy of rotating stall is 97%. The accurate identification of rotating stall of centrifugal compressor is realized, which lays a foundation for the intelligent operation and maintenance of centrifugal compressor.

The identification accuracy of the proposed method for similar flow conditions is about 85%. Future research will further enhance the performance of the proposed method, and the parameter will be further optimized.

Acknowledgments

The presented research was supported through the Joint Funds of the National Natural Science Foundation of China (Grant No. U1808214), National Key Research and Development Project (Grant No. 2020YFB2010800), and the National Natural Science Foundation of China (Grant No. 92060105).

CONFLICT OF INTEREST STATEMENT

The authors declare no conflicts of interest.

References

1. X. Xue and T. Wang, "Stall recognition for centrifugal compressors during speed transients," *Appl. Therm. Eng.*, vol. 153, pp. 104–112, 2019.
2. Q. Zhang et al., "Study on two types of stall patterns in a centrifugal compressor with a wide vaneless diffuser," *Processes*, vol. 8, p. 1251, 2020.
3. L. Zhang, R. He, S. Wang, and Q. Zhang, "A review of rotating stall in vaneless diffuser of centrifugal compressor," *J. Therm. Sci.*, vol. 29, pp. 323–342, 2020.
4. Y. V. Kozhukhov et al., "Identification of rotating stall zones and the velocity of their movement in a centrifugal compressor," in AIP Conf. Proc., ICSAS, pp. 2285–2294, 2020.
5. S. Zhou, J. Jin, and Y. Wei, "Research on online diagnosis method of fuel cell centrifugal air compressor surge fault," *Energies*, vol. 14, p. 3071, 2021.
6. N. Zhang et al., "Coherence analysis to detect unsteady rotating stall phenomenon based on pressure pulsation signals of a centrifugal pump," *Mech. Syst. Signal Process.*, vol. 148, p. 107161, 2021.
7. H. Zhang, C. Yang, D. Yang, Y. Li, and C. Yang, "Investigation of stall inception behavior in a centrifugal compressor with bent pipe/volute coupling effect," *J. Propul. Power*, vol. 35, pp. 382–395, 2019.
8. A. Zamiri, M. Choi, and J. Taek Chung, "Numerical investigation of rotating stall characteristics in a full-annulus transonic centrifugal compressor," *J. Propul. Power*, vol. 37, pp. 369–380, 2021.
9. L. Zhang, Z. Zheng, Q. Zhang, L. Zhang, and K. Li, "Study of rotating stall in a centrifugal compressor with wide vaneless diffuser," *J. Therm. Sci.*, vol. 29, pp, 743–752, 2020.
10. A. Ghenaiet and S. Khalfallah, "Assessment of some stall-onset criteria for centrifugal compressors," *Aerosp. Sci. Technol.*, vol. 88, pp. 193–207, 2019.
11. J. Lu et al., "Detection of the flow state for a centrifugal pump based on vibration," *Energies*, vol. 12, p. 3066, 2019.
12. X. Zhao et al., "Rotating stall induced non-synchronous blade vibration analysis for an unshrouded industrial centrifugal compressor," *Sensors-Basel*, vol. 19, p. 4995, 2019.
13. N. Fujisawa, T. Inui, and Y. Ohta, "Evolution process of diffuser stall in a centrifugal compressor with vaned diffuser," *ASME. J. Turbomach.*, vol. 141, no. 4, p. 041009, Apr. 2019.
14. J. Yu, X. Zheng, and S. Wang, "A deep autoencoder feature learning method for process pattern recognition," *J. Process Control*, vol. 79, pp. 1–15, 2019.
15. J. Yu, "Manifold regularized stacked denoising autoencoders with feature selection," *Neurocomputing*, vol. 358, pp. 235–245, 2019.
16. H. Shao et al., "A novel deep autoencoder feature learning method for rotating machinery fault diagnosis," *Mech. Syst. Signal Process.*, vol. 95, pp. 187–204, 2017.
17. Z. Meng et al., "An enhancement denoising autoencoder for rolling bearing fault diagnosis," *Measurement*, vol. 130, pp. 448–454, 2018.
18. M. Sun et al., "A sparse stacked denoising autoencoder with optimized transfer learning applied to the fault diagnosis of rolling bearings," *Measurement*, vol. 146, pp. 305–314, 2019.
19. A. Law and A. Ghosh, "Multi-label classification using a cascade of stacked autoencoder and extreme learning machines," *Neurocomputing*, vol. 358, pp. 222–234, 2019.
20. S. Lin, J. Zeng, and X. Chang, "Learning rates for classification with gaussian kernels," *Neural Comput.*, vol. 29, no. 12, pp. 3353–3380, 2017.
21. X. Zhang, X. Liu, Z. J. Wang, "Evaluation of a set of new ORF kernel functions of SVM for speech recognition," *Eng. Appl. Artif. Intel.*, vol. 26, pp. 2574–2580, 2013.
22. H. Zhang et al., "Investigation of stall inception behavior in a centrifugal compressor with bent pipe/volute," *Coupling Effect. J. Propul. Power*, vol. 35, pp. 382–395, 2019.